JOURNAL OF GUIDANCE, CONTROL, AND DYNAMICS
Vol. 19, No. 3, May–June 1996

Analytical Solution of Three-Dimensional Realistic True Proportional Navigation

Ciann-Dong Yang and Chi-Ching Yang
National Cheng Kung University, Tainan 701, Taiwan, Republic of China

True proportional navigation with varying closing speed is called realistic true proportional navigation, which is implemented in practice. Our main goal is to derive the complete solutions of three-dimensional realistic true proportional navigation for nonmaneuvering and maneuvering targets. Three coupled nonlinear second-order state equations describing the relative motion are solved analytically without any linearization for performance and trajectory analysis. Properties of three-dimensional realistic true proportional navigation such as capture region, range-to-go, time-to-go, and two aspect angles within spherical coordinates are all obtained in closed form. Furthermore, the two-player game between three-dimensional realistic true proportional navigation and three-dimensional ideal proportional navigation is investigated analytically in the pursuit–evasion scenario, where a realistic true proportional navigation guided missile is designed to pursue an ideal proportional navigation guided target. It is found that an ideal proportional navigation guided target is much harder to intercept than a realistic true proportional navigation guided target.

I. Introduction

PROPORTIONAL navigation (PN) for short-range tactical missiles is the optimal interceptive law in the sense of producing zero miss distance with the least integral square control effort. PN has been studied since the 1940s. During the four decades that followed, proportional navigation has been explored in many different ways, such as true proportional navigation, pure proportional navigation (PPN), generalized proportional navigation, realistic true proportional navigation (RTPN), and ideal proportional navigation (IPN).[1–20]

It has long been recognized that there exists a significant difference in the way in which PN guidance law is analyzed and in the way in which it is implemented. Most analytical studies of PN assume that the closing velocity in the PN guidance law is constant, whereas in realistic situations, the instantaneous closing speed may be continuously estimated or measured using devices such as homing seekers with Doppler radar. To remove this difference, RTPN, which adapts to varying closing speed, has recently been proposed. Performance and trajectory analysis of two-dimensional RTPN was studied by Yuan and Chern,[14] and the capture region of RTPN was investigated by Ghose[19] and Dhar and Ghose.[17] Degradation in the capture region for RTPN has been observed.

Because of the difficulties in analysis, most analytical studies on PN guidance laws in the past used two-dimensional models, although actual pursuit–evasion motion occurred in a three-dimensional environment. As for three-dimensional studies, earlier work was done by Adler.[21] The main viewpoint of his study was that the three-dimensional relative motion can be described by the principle plane defined by the instantaneous line of sight (LOS) and by the missile's velocity. Shinar et al.[22] used the linearized three-dimensional model to analyze guidance laws. Guelman and Shinar[23] extended the optimal guidance law in the plane to three-dimensional models and obtained a preliminary version of three-dimensional optimal guidance law. Cochran et al.[24] considered the three-dimensional RTPN guidance problem; a partial solution has been revealed. More recently, Yang and Yang[25] proposed a systematic solution technique for three-dimensional guidance laws, and the technique has been applied to generalized three-dimensional

Ciann-Dong Yang received his B.S., M.S., and Ph.D. degrees in aeronautics and astronautics from National Cheng Kung University, Taiwan, in 1983, 1985, and 1987, respectively. Since 1985, he has been with the Department of Aeronautics and Astronautics, National Cheng Kung University, where he is currently an Associate Professor. His research interests are in H_∞ robust control and missile guidance. Dr. Yang is the recipient of the 1990 M. Barry Carlton Award and the Outstanding Paper Award of the IEEE Aerospace and Electronic Systems. He is also the author of *Engineering Analysis* and is the coauthor of *Post Modern Control Theory and Design*.

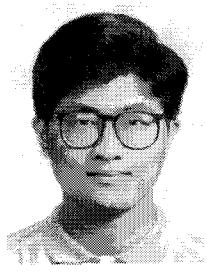

Chi-Ching Yang received his B.S. degree in mechanical engineering from Chung Yuan University, Taiwan, in 1991 and his M.S. degree in aeronautics and astronautics from National Cheng Kung University, Taiwan, in 1993. He is currently a Ph.D. candidate in the Institute of Aeronautics and Astronautics, National Cheng Kung University, Taiwan. His research interests are mainly in missile three-dimensional guidance and control theory.

Received June 1, 1995; revision received Oct. 23, 1995; accepted for publication Nov. 8, 1995.

proportional navigation problems; complete solutions to the three coupled nonlinear differential equations within spherical coordinates were obtained without any linearization.

The discussion of the two-dimensional PN guidance law had used moving polar coordinates wherein the origin is fixed on the missile to characterize the relative motion. In three-dimensional models, seeker measurements are spherical in nature[26] (range and angles) and are, therefore, nonlinear functions of the state in Cartesian coordinates. The nonlinear transformation of states could be avoided if the guidance laws were formulated in spherical coordinates. Thus, moving spherical coordinates seem to be most natural in characterizing three-dimensional relative motions.

Hence, we will use spherical coordinates to describe the relative motion of a target with respect to the missile that is the origin of the moving coordinates and is guided by three-dimensional RTPN. The resulting relative motion is governed by three second-order nonlinear differential equations whose solution has never been discussed before. Based on the systematic framework[25] for analyzing three-dimensional guidance laws, we have made a breakthrough in obtaining the analytical solutions of these coupled nonlinear differential equations that are derived in terms of the unit angular momentum defined by the relative motion. Unit angular momentum in the space is an index measuring the departure tendency of the three-dimensional relative motion from a fixed plane. If the relative motion occurs wholly within a fixed plane, then the direction of the relative angular momentum will remain constant during the course of interception. Besides as an index for measuring three-dimensional relative motions, unit angular momentum can be used to establish a new moving coordinate that has a decoupling effect such that the relative distance and azimuths can be solved independently.

Systematic frameworks for analyzing three-dimensional guidance laws are introduced in Sec. II. Three-dimensional RTPN is defined in Sec. III, where three nonlinear differential equations describing the relative motion with respect to a nonmaneuvering target are solved analytically, and the trajectory properties such as capture region, time-to-go, range-to-go, and aspect angles are all derived in closed forms. In Sec. IV, we solve the two-player-game problem wherein a missile guided by three-dimensional RTPN is designed to pursue a target guided by three-dimensional IPN. Numerical results and additional physical insight about the three-dimensional RTPN guidance law are discussed in Sec. V.

II. General Analysis of Three-Dimensional Relative Motion

Consider the spherical coordinates (r, θ, ϕ) with origin fixed at the missile, where r is the relative distance between missile and target and θ and ϕ are azimuths. Let $(\boldsymbol{e}_r, \boldsymbol{e}_\theta, \boldsymbol{e}_\phi)$ be unit vectors along the coordinate axes (see Fig. 1). According to the principles of kinematics, the three relative acceleration components (a_r, a_θ, a_ϕ) can be expressed by the following set of second-order nonlinear differential equations:

$$\ddot{r} - r\dot{\phi}^2 - r\dot{\theta}^2\cos^2\phi = a_{T_r} - a_{M_r} \equiv a_r \tag{1a}$$

$$r\ddot{\theta}\cos\phi + 2\dot{r}\dot{\theta}\cos\phi - 2r\dot{\phi}\dot{\theta}\sin\phi = a_{T_\theta} - a_{M_\theta} \equiv a_\theta \tag{1b}$$

$$r\ddot{\phi} + 2\dot{r}\dot{\phi} + r\dot{\theta}^2\cos\phi\sin\phi = a_{T_\phi} - a_{M_\phi} \equiv a_\phi \tag{1c}$$

where a_{T_r}, a_{T_θ}, and a_{T_ϕ} are the acceleration components of the target and a_{M_r}, a_{M_θ}, and a_{M_ϕ} are the acceleration components for the missile. To analyze these coupled nonlinear equations, we find that the exploitation of the angular momentum of unit mass is very helpful. The unit angular momentum $\boldsymbol{h}$ for the missile-target relative motion is defined as

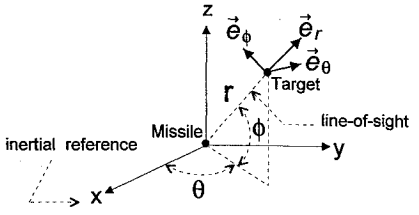

Fig. 1 Three-dimensional pursuit geometry.

$$\boldsymbol{h} = \boldsymbol{r} \times \dot{\boldsymbol{r}} \tag{2}$$

where $\boldsymbol{r}$ is the relative displacement along the LOS and $\dot{\boldsymbol{r}}$ is the relative velocity. Accordingly, if the relative motion occurs within a fixed plane, i.e., $\boldsymbol{r}$ and $\dot{\boldsymbol{r}}$ are in the same plane during the interception, then the direction of $\boldsymbol{h}$ will be constant: always perpendicular to the plane spanned by $\boldsymbol{r}$ and $\dot{\boldsymbol{r}}$. Hence, the variation of the direction of $\boldsymbol{h}$ is a natural measure for departure tendency of the relative motion from a fixed plane.

Here, $\boldsymbol{r}$ and $\dot{\boldsymbol{r}}$ can be expressed by the spherical unit vectors $(\boldsymbol{e}_r, \boldsymbol{e}_\theta, \boldsymbol{e}_\phi)$ as

$$\boldsymbol{r} = r\boldsymbol{e}_r \tag{3a}$$

$$\dot{\boldsymbol{r}} = \dot{r}\boldsymbol{e}_r + r\dot{\theta}\cos\phi\boldsymbol{e}_\theta + r\dot{\phi}\boldsymbol{e}_\phi \tag{3b}$$

Substituting Eqs. (3) into Eq. (2) yields the expression for $\boldsymbol{h}$,

$$\boldsymbol{h} = h\boldsymbol{e}_h = r^2(-\dot{\phi}\boldsymbol{e}_\theta + \dot{\theta}\cos\phi\boldsymbol{e}_\phi) \tag{4a}$$

where

$$h = r^2\sqrt{\dot{\phi}^2 + \dot{\theta}^2\cos^2\phi} \tag{4b}$$

is the magnitude of $\boldsymbol{h}$ and

$$\boldsymbol{e}_h = (r^2/h)(-\dot{\phi}\boldsymbol{e}_\theta + \dot{\theta}\cos\phi\boldsymbol{e}_\phi) \tag{4c}$$

is the unit vector along the direction of $\boldsymbol{h}$. According to the definition of $\boldsymbol{e}_h$, we know that $\boldsymbol{e}_h$ is perpendicular to $\boldsymbol{e}_r$. We can find another unit vector $\boldsymbol{e}_h^\perp$ that is perpendicular to both $\boldsymbol{e}_r$ and $\boldsymbol{e}_h$. It is straightforward to verify

$$\boldsymbol{e}_h^\perp = (r^2/h)(\dot{\theta}\cos\phi\boldsymbol{e}_\theta + \dot{\phi}\boldsymbol{e}_\phi) \tag{5}$$

The set of unit vectors $(\boldsymbol{e}_r, \boldsymbol{e}_h^\perp, \boldsymbol{e}_h)$ constitutes a new moving coordinate system that is more convenient for describing three-dimensional guidance laws than the conventional spherical coordinates $(\boldsymbol{e}_r, \boldsymbol{e}_\theta, \boldsymbol{e}_\phi)$, as will be seen later.

We now proceed to derive the various physical components under the new coordinate system $(\boldsymbol{e}_r, \boldsymbol{e}_h^\perp, \boldsymbol{e}_h)$. The differentiation of Eq. (2) gives

$$\frac{\mathrm{d}\boldsymbol{h}}{\mathrm{d}t} = \boldsymbol{r} \times \ddot{\boldsymbol{r}} \tag{6}$$

where $\ddot{\boldsymbol{r}}$ is the relative acceleration defined by

$$\ddot{\boldsymbol{r}} = a_r\boldsymbol{e}_r + a_\theta\boldsymbol{e}_\theta + a_\phi\boldsymbol{e}_\phi \tag{7}$$

Using Eqs. (3a) and (7), the right-hand side of Eq. (6) can be rewritten as

$$\boldsymbol{r} \times \ddot{\boldsymbol{r}} = (-ra_\phi)\boldsymbol{e}_\theta + (ra_\theta)\boldsymbol{e}_\phi \tag{8}$$

and the left-hand side of Eq. (6) becomes

$$\frac{\mathrm{d}}{\mathrm{d}t}(\boldsymbol{h}) = \dot{h}\boldsymbol{e}_h + h\dot{\boldsymbol{e}}_h \tag{9}$$

where $\dot{h}$ and $\dot{\boldsymbol{e}}_h$ can be obtained from the differentiation of Eqs. (4b) and (4c) with respect to time t. Upon differentiating h and $\boldsymbol{e}_h$, we need the relations

$$\dot{\boldsymbol{e}}_r = \boldsymbol{\omega} \times \boldsymbol{e}_r, \qquad \dot{\boldsymbol{e}}_\theta = \boldsymbol{\omega} \times \boldsymbol{e}_\theta, \qquad \dot{\boldsymbol{e}}_\phi = \boldsymbol{\omega} \times \boldsymbol{e}_\phi$$

where $\boldsymbol{\omega}$ is the angular velocity of the moving coordinates $(\boldsymbol{e}_r, \boldsymbol{e}_\theta, \boldsymbol{e}_\phi)$ that can be derived as

$$\boldsymbol{\omega} = \dot{\theta}\sin\phi\boldsymbol{e}_r - \dot{\phi}\boldsymbol{e}_\theta + \dot{\theta}\cos\phi\boldsymbol{e}_\phi \tag{10}$$

and $\dot{h}$ and $\dot{\boldsymbol{e}}_h$ are found as follows:

$$\dot{h} = \frac{2r\dot{r}(\dot{\phi}^2 + \dot{\theta}^2\cos^2\phi) + r^2(\ddot{\theta}\dot{\theta}\cos^2\phi - \dot{\phi}\dot{\theta}^2\sin\phi\cos\phi + \dot{\phi}\ddot{\phi})}{\sqrt{\dot{\phi}^2 + \dot{\theta}^2\cos^2\phi}} \tag{11a}$$

$$\dot{\boldsymbol{e}}_h = \frac{1}{\sqrt{\dot{\phi}^2 + \dot{\theta}^2\cos^2\phi}} \times \left[\left(-\ddot{\phi} + \frac{\dot{\phi}(\dot{\phi}\ddot{\phi} + \dot{\theta}\ddot{\theta}\cos^2\phi - \dot{\theta}^2\dot{\phi}\sin\phi\cos\phi)}{\dot{\phi}^2 + \dot{\theta}^2\cos^2\phi} - \dot{\theta}^2\sin\phi\cos\phi\right)\boldsymbol{e}_\theta + \left(\ddot{\theta}\cos\phi - \dot{\theta}\dot{\phi}\sin\phi - \frac{\dot{\theta}\cos\phi(\dot{\phi}\ddot{\phi} + \dot{\theta}\ddot{\theta}\cos^2\phi - \dot{\theta}^2\dot{\phi}\sin\phi\cos\phi)}{\dot{\phi}^2 + \dot{\theta}^2\cos^2\phi} - \dot{\theta}\dot{\phi}\sin\phi\right)\boldsymbol{e}_\phi\right] \tag{11b}$$

Equations (11) are substituted into Eq. (9) to obtain

$$\frac{\mathrm{d}}{\mathrm{d}t}(\boldsymbol{h}) = -r(r\ddot{\phi} + 2\dot{r}\dot{\phi} + r\dot{\theta}^2\cos\phi\sin\phi)\boldsymbol{e}_\theta + r(r\ddot{\theta}\cos\phi + 2\dot{r}\dot{\theta}\cos\phi - 2r\dot{\phi}\dot{\theta}\sin\phi)\boldsymbol{e}_\phi \tag{12}$$

If we equate Eq. (6) with Eq. (12), we go back to the results of Eqs. (1b) and (1c); however, this fact manifests that the roles of Eqs. (1b) and (1c) can be replaced by the roles of Eqs. (11) in describing the relative motion. Equations (11) can be further simplified to the following form:

$$\dot{h} = \boldsymbol{r}\cdot(\dot{\boldsymbol{r}}\times\boldsymbol{e}_h) = (r^3/h)(a_\phi\dot{\phi} + a_\theta\dot{\theta}\cos\phi) \tag{13a}$$

$$\dot{\boldsymbol{e}}_h = (r/h)(\dot{\boldsymbol{r}}\cdot\boldsymbol{e}_h)\boldsymbol{e}_h^\perp = (r^3/h^2)(a_\theta\dot{\phi} - a_\phi\dot{\theta}\cos\phi)\boldsymbol{e}_h^\perp \tag{13b}$$

The remaining equation describing the relative motion comes from Eq. (1a), that can be rewritten in terms of h as

$$\ddot{r} - (h^2/r^3) = a_r \tag{13c}$$

Equations (13) are equivalent to Eqs. (1), but Eqs. (13) have the advantage of decoupling the radial motion from the tangential motion as can be seen in the following sections.

III. Three-Dimensional RTPN with Nonmaneuvering Targets

In the two-dimensional case, RTPN is so called because acceleration of the missile is proportional to the angular velocity $\boldsymbol{\Omega}$ of LOS ($\boldsymbol{r}$) and proportional to the instantaneous closing velocity $\dot{r}\boldsymbol{e}_r$. In the three-dimensional case, the commanded missile acceleration $\boldsymbol{a}_M$ can be readily extended to the vector form

$$\boldsymbol{a}_M = \lambda\dot{r}\boldsymbol{e}_r \times \boldsymbol{\Omega} \tag{14a}$$

where λ is the proportional navigation gain. The angular velocity $\boldsymbol{\Omega}$ of $\boldsymbol{r}$ can be found from the relation

$$\boldsymbol{\Omega} = (\boldsymbol{r}\times\dot{\boldsymbol{r}})/r^2 = \boldsymbol{h}/r^2 = -\dot{\phi}\boldsymbol{e}_\theta + \dot{\theta}\cos\phi\boldsymbol{e}_\phi \tag{14b}$$

where Eq. (4a) has been used to obtain Eq. (14b). Therefore, missile acceleration becomes

$$\boldsymbol{a}_M = \lambda\dot{r}\boldsymbol{e}_r \times (\boldsymbol{h}/r^2) = -\lambda(\boldsymbol{h}\dot{r}/r^2)\boldsymbol{e}_h^\perp \tag{15}$$

In this section only a nonmaneuvering target is assumed, i.e., $\boldsymbol{a}_T = 0$. After substituting Eq. (15) into Eqs. (13), we have

$$\ddot{r} - (h^2/r^3) = 0 \tag{16a}$$

$$\dot{h} = \lambda h(\dot{r}/r) \tag{16b}$$

$$\dot{\boldsymbol{e}}_h = 0 \tag{16c}$$

Equations (16a) and (16b) can be solved together, leading to the following results:

$$h = h_0(r/r_0)^\lambda \tag{17}$$

$$\dot{r} = -\sqrt{\dot{r}_0^2 - \frac{h_0^2/r_0^2}{\lambda - 1} + \frac{h_0^2/r_0^{2\lambda}}{\lambda - 1}r^{2\lambda - 2}} \tag{18}$$

Combining Eqs. (14b) and (17) yields

$$\Omega = h/r^2 = \left(h_0/r_0^2\right)(r/r_0)^{\lambda - 2} \tag{19}$$

To maintain finite commanded acceleration, the navigation constant λ must be greater than 2. The capture area of three-dimensional RTPN can be evaluated from the terminal condition: $r(t_f) = 0$, $\dot{r}(t_f) < 0$. From Eq. (18) we find that for a successful interception, the initial conditions must fall within the following range:

$$\frac{|\dot{r}_0|}{h_0/r_0} > \frac{1}{\sqrt{\lambda - 1}} \tag{20}$$

To have the analytical solution independent of the initial conditions, a nondimensionalized process is required before we proceed further. Dimensionless variables are defined as follows:

$$\rho = \frac{r}{r_0}, \qquad \tau = \frac{t}{r_0/V_0}, \qquad \bar{h} = \frac{h}{r_0 V_0} \tag{21}$$

where $V_0 = |\dot{r}_0|$ is the initial relative speed defined as $V_0 = \sqrt{(\dot{r}_0^2 + h_0^2/r_0^2)}$. With the help of these dimensionless variables, the capture region defined by Eq. (20) can be rewritten in a more compact form as

$$\bar{h}_0 < \sqrt{1 - (1/\lambda)} \tag{22}$$

Unlike the conventional expression of the capture region[5,14,17] that was defined in the two-parameter space (V_{r_0}, V_{θ_0}), here we can see that capture region can, indeed, be defined by using only one parameter: unit angular momentum $\bar{h}_0$.

The dimensionless forms of Eqs. (17) and (18) become

$$\bar{h} = \bar{h}_0\rho^\lambda \tag{23}$$

$$\frac{\mathrm{d}\rho}{\mathrm{d}\tau} = -\sqrt{\frac{\dot{r}_0^2}{V_0^2} + \frac{\bar{h}_0^2}{\lambda - 1}(\rho^{2\lambda - 2} - 1)} \tag{24}$$

The integration of Eq. (24) then gives the relation between normalized range to go ρ and normalized forward time τ,

$$\tau = -\int_1^\rho \frac{\mathrm{d}\rho}{\sqrt{\dot{r}_0^2/V_0^2 + \left[\bar{h}_0^2/(\lambda - 1)\right](\rho^{2\lambda - 2} - 1)}} \tag{25}$$

The duration of interception can be found as

$$\tau_f = \int_0^1 \frac{\mathrm{d}\rho}{\sqrt{\dot{r}_0^2/V_0^2 + \left[\bar{h}_0^2/(\lambda - 1)\right](\rho^{2\lambda - 2} - 1)}} \tag{26}$$

The commanded missile acceleration can be calculated from Eq. (15):

$$\frac{a_M}{V_0^2/r_0} = \lambda\bar{h}\rho^{-2}\frac{\mathrm{d}\rho}{\mathrm{d}\tau} = \lambda\bar{h}_0\rho^{\lambda - 2}\sqrt{\dot{r}_0^2/V_0^2 + \left[\bar{h}_0^2/(\lambda - 1)\right](\rho^{2\lambda - 2} - 1)} \tag{27}$$

The total normalized cumulative velocity increment ΔV of the missile during interception is defined as

$$\Delta V = \int_0^{\tau_f} \left|\frac{a_M}{V_0^2/r_0}\right| \mathrm{d}\tau \tag{28}$$

Substituting Eqs. (24) and (27) into Eq. (28), we have

$$\Delta V = \int_0^1 \lambda \bar{h}_0 \rho^{\lambda-2}\, d\rho = \frac{\lambda}{\lambda-1}\bar{h}_0 \tag{29}$$

There are three time functions, $\rho(t)$, $\theta(t)$, and $\phi(t)$, needed to describe the three-dimensional relative motion within the spherical coordinates. Up to this stage, only relative distance $\rho(t)$ is obtained. The following work is to find the azimuths $\theta(t)$ and $\phi(t)$. This step is much harder than the solution of r. The problem is attacked starting from Eq. (16c). Substituting Eq. (11b) into Eq. (16c) and using the transformation between the two coordinate systems $(\boldsymbol{e}_r, \boldsymbol{e}_\theta, \boldsymbol{e}_\phi)$ and $(\boldsymbol{e}_r, \boldsymbol{e}_h^\perp, \boldsymbol{e}_h)$, we obtain the key equation characterizing the behavior of $\theta(t)$ and $\phi(t)$ as

$$\frac{\ddot{\theta}\cos\phi - \dot{\theta}\dot{\phi}\sin\phi}{-\dot{\phi}} + \frac{\dot{\theta}\cos\phi(\ddot{\theta}\dot{\theta}\cos^2\phi - \dot{\phi}\dot{\theta}^2\sin\phi\cos\phi + \phi\ddot{\phi})}{\dot{\phi}(\dot{\phi}^2 + \dot{\theta}^2\cos^2\phi)} + \dot{\theta}\sin\phi = 0 \tag{30}$$

This equation can be simplified to a totally differentiable form:

$$\frac{d(\dot{\theta}\cos\phi)}{-\dot{\theta}\cos\phi} + \frac{d(\dot{\phi}^2 + \dot{\theta}^2\cos^2\phi)}{2(\dot{\phi}^2 + \dot{\theta}^2\cos^2\phi)} + \tan\phi\, d\phi = 0$$

and the integration gives

$$\frac{\dot{\phi}^2 + \dot{\theta}^2\cos^2\phi}{\dot{\theta}^2\cos^4\phi} = \frac{\dot{\phi}_0^2 + \dot{\theta}_0^2\cos^2\phi_0}{\dot{\theta}_0^2\cos^4\phi_0} = l^2 \tag{31}$$

where l is an integration constant. The preceding equation can be solved for $\dot{\phi}^2$ in terms of $\dot{\theta}^2$:

$$\left(\frac{d\phi}{d\tau}\right)^2 = (l^2\cos^4\phi - \cos^2\phi)\left(\frac{d\theta}{d\tau}\right)^2 \tag{32}$$

The other relation between $d\phi/d\tau$ and $d\theta/d\tau$ comes from Eq. (4b):

$$\bar{h}^2 = \rho^4\left[\left(\frac{d\phi}{d\tau}\right)^2 + \left(\frac{d\theta}{d\tau}\right)^2\cos^2\phi\right] \tag{33}$$

Substituting Eqs. (23) and (32) into Eq. (33) yields

$$\left(\frac{d\theta}{d\tau}\right)^2 = \left(\frac{\bar{h}_0}{l}\right)^2\rho^{2\lambda}(\rho\cos\phi)^{-4} \tag{34}$$

which, in turn, is substituted into Eq. (32) to obtain the expression for $d\phi/d\tau$ as

$$\frac{d\phi}{d\tau} = \text{sign}(\dot{\phi}_0)\,\bar{h}_0\rho^{\lambda-2}\sqrt{1 - l^{-2}\cos^{-2}\phi} \tag{35}$$

The relation between ϕ and ρ can be obtained by integrating Eq. (35) with the help of Eq. (24):

$$\int_0^\phi \frac{d\phi}{\sqrt{1 - l^{-2}\cos^{-2}\phi}} = \text{sign}(\dot{\phi}_0)\int_\rho^1 \frac{\bar{h}_0\rho^{\lambda-2}d\rho}{\sqrt{\left(\dot{r}_0^2/V_0^2\right) + \left[\bar{h}_0^2/(\lambda-1)\right](\rho^{2\lambda-2} - 1)}} \tag{36}$$

The remaining step is to relate θ to ϕ by integrating Eq. (32):

$$\theta = \text{sign}\left(\frac{\dot{\theta}_0}{\dot{\phi}_0}\right)\int_0^\phi \frac{d\phi}{\cos^2\phi\sqrt{l^2 - \cos^{-2}\phi}} \tag{37}$$

It can be observed from Eqs. (35) and (37) that both $\theta(\tau)$ and $\phi(\tau)$ are monotonically increasing when $\dot{\theta}_0 > 0$ and $\dot{\phi}_0 > 0$, whereas both $\theta(\tau)$ and $\phi(\tau)$ are monotonically decreasing when $\dot{\theta}_0 < 0$ and $\dot{\phi}_0 < 0$. Without loss of generality, we will assume $\theta_0 = 0$, $\phi_0 = 0$, $\dot{\theta}_0 > 0$, and $\dot{\phi}_0 > 0$ in the following discussion. These initial conditions can be naturally achieved by choosing the inertial reference line as the initial LOS and by defining the positive directions of θ and ϕ as the directions of $\dot{\theta}_0$ and $\dot{\phi}_0$.

To express the solutions more explicitly, we find that the introduction of the following auxiliary azimuths ψ and η is very helpful. The first auxiliary azimuth ψ is defined as

$$\frac{\cos\psi}{\cos\psi_0} = \rho^{\lambda-1} \tag{38}$$

where $\psi_0 = \cos^{-1}C$ and C is defined as

$$C = \frac{1}{\sqrt{\lambda-1}}\left(\frac{\bar{h}_0}{|\dot{r}_0/V_0|}\right) = \frac{\bar{h}_0}{\sqrt{(\lambda-1)\left(1 - \bar{h}_0^2\right)}} \tag{39}$$

When interpreted in terms of C, the capture region defined in Eq. (22) is equivalent to the condition $C < 1$.

The second auxiliary azimuth η is defined as

$$\frac{\cos\eta}{\cos\eta_0} = \frac{1}{\cos\phi} \tag{40}$$

where $\cos\eta_0 = 1/l = \dot{\theta}_0/\sqrt{(\dot{\theta}_0^2 + \dot{\phi}_0^2)} \le 1$. Instead of normalized time τ and range to go ρ, we find that ψ and η are more appropriate for use as independent variables to describe the three-dimensional relative motion. Parameters $\bar{h}$, ρ, τ, ϕ, and θ can all be expressed by ψ and η. From Eqs. (23) and (38), we have

$$\bar{h}/\bar{h}_0 = \left(\frac{\cos\psi}{\cos\psi_0}\right)^{\lambda/(\lambda-1)} \tag{41}$$

The relation between time τ and ψ is established by substituting Eq. (38) into Eq. (25). After some manipulations, we have

$$\tau = \frac{1}{|\dot{r}_0|/V_0}\int_\rho^1 \frac{d\rho}{\sqrt{\sin^2\psi_0 + \cos^2\psi_0\rho^{2\lambda-2}}} \tag{42}$$

The required time of interception is attained by setting $\rho = 0$ in the lower limit of the preceding integration:

$$\tau_f = \frac{1}{|\dot{r}_0|/V_0}\int_0^1 \frac{d\rho}{\sqrt{\sin^2\psi_0 + \cos^2\psi_0\rho^{2\lambda-2}}} \tag{43}$$

This integration can be expressed by elliptic functions. Azimuth ϕ is related to ψ by substituting Eq. (38) into Eq. (36), leading to the following identity:

$$\frac{1}{\sqrt{\lambda-1}}\int_{\cos\psi}^{\cos\psi_0} \frac{d(\cos\psi)}{\sqrt{\sin^2\psi_0 + \cos^2\psi}} = \int_0^\phi \frac{d\phi}{\sqrt{1 - l^{-2}\cos^{-2}\phi}} \tag{44a}$$

The integrations involved in Eq. (44a) can be evaluated in terms of elementary functions, leading to the following explicit formula:

$$\phi = \sin^{-1}\left\{\sqrt{1 - l^{-2}}\times\sin\left[\frac{\sinh^{-1}\cot\psi_0 - \sinh^{-1}(\cos\psi/\sin\psi_0)}{\sqrt{\lambda-1}}\right]\right\} \tag{44b}$$

On the other hand, θ is related to η by substituting Eq. (40) into Eq. (37):

$$\theta = -\int_{\eta_0}^\eta \frac{\cos\eta\, d\eta}{\sqrt{\cos^2\eta - l^{-2}}} = \cos^{-1}\left(\frac{\sin\eta}{\sin\eta_0}\right) \tag{45}$$

The auxiliary azimuth η has a concrete physical meaning. Combining Eqs. (31) and (40), we can show that

$$\sin\eta = \frac{\dot{\phi}}{\sqrt{\dot{\phi}^2 + \dot{\theta}^2\cos^2\phi}}, \qquad \cos\eta = \frac{\dot{\theta}\cos\phi}{\sqrt{\dot{\phi}^2 + \dot{\theta}^2\cos^2\phi}} \tag{46}$$

Substituting Eqs. (46) into Eq. (4c) yields

$$\boldsymbol{e}_h = -\sin\eta\,\boldsymbol{e}_\theta + \cos\eta\,\boldsymbol{e}_\phi \tag{47}$$

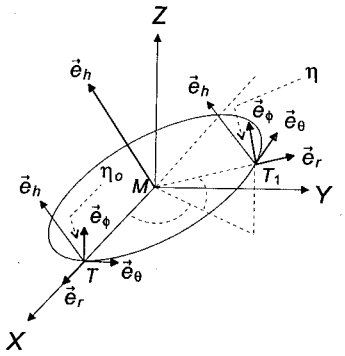

Fig. 2 Angle η between e_h and e_ϕ.

This reveals that η is the angle between $\boldsymbol{e}_h$ and $\boldsymbol{e}_\phi$, as shown in Fig. 2. As mentioned earlier, $\boldsymbol{e}_h$ is normal to the instantaneous plane spanned by $\boldsymbol{r}$ and $\dot{\boldsymbol{r}}$. Consequently, when the relative motion remains within a fixed plane in the three-dimensional space, the direction of $\boldsymbol{e}_h$ will not change. This is what we have derived in Eq. (16c). In the following we will show that when a nonmaneuvering target is pursued by a missile guided by three-dimensional RTPN guidance law, the whole relative motion, indeed, occurs within a fixed plane, but this plane may not be limited to the horizontal x–y plane. To show $\boldsymbol{e}_h$ is fixed in the three-dimensional space, the most natural way is to express $\boldsymbol{e}_h$ in terms of the inertial coordinates $(\boldsymbol{i}, \boldsymbol{j}, \boldsymbol{k})$, and to show that the components of $\boldsymbol{e}_h$ in the $\boldsymbol{i}$, $\boldsymbol{j}$, and $\boldsymbol{k}$ directions are all constant.

Exploiting the transformation between the spherical coordinates and the inertial Cartesian coordinates,

$$\boldsymbol{e}_\theta = -\sin\theta\boldsymbol{i} + \cos\theta\boldsymbol{j}$$

$$\boldsymbol{e}_\phi = -\sin\phi\cos\theta\boldsymbol{i} - \sin\phi\sin\theta\boldsymbol{j} + \cos\phi\boldsymbol{k}$$

we can express $\boldsymbol{e}_h$ of Eq. (47) in terms of the inertial Cartesian coordinates as

$$\boldsymbol{e}_h = (\sin\eta\sin\theta - \cos\eta\sin\phi\cos\theta)\boldsymbol{i} + (-\sin\eta\cos\theta - \cos\eta\sin\phi\sin\theta)\boldsymbol{j} + (\cos\eta\cos\phi)\boldsymbol{k} \quad (48)$$

The simplification of Eq. (48) needs two relations from Eqs. (40) and (45):

$$\cos\theta = \frac{\sin\eta}{\sin\eta_0}, \qquad \sin\theta = \cot\eta_0\tan\phi \quad (49)$$

Using Eqs. (40) and (49), we can establish the following identities:

$$\sin\eta\sin\theta - \cos\eta\sin\phi\cos\theta = 0 \quad (50a)$$

$$-\sin\eta\cos\theta - \cos\eta\sin\phi\sin\theta = -\sin\eta_0 \quad (50b)$$

$$\cos\eta\cos\phi = \cos\eta_0 \quad (50c)$$

Therefore, Eq. (48) becomes

$$\boldsymbol{e}_h = -\sin\eta_0\boldsymbol{j} + \cos\eta_0\boldsymbol{k} \quad (51)$$

As expected, $\boldsymbol{e}_h$ is fixed in the inertial coordinates and the constant orientation of the plane where the relative motion occurs is determined by η_0 that is defined by the initial angular rates as

$$\eta_0 = \cos^{-1}\sqrt{\frac{\dot\theta_0^2}{\dot\theta_0^2 + \dot\phi_0^2}}$$

Since we have chosen $\theta_0 = 0$ and $\phi_0 = 0$, the moving spherical coordinates coincide with the inertial Cartesian coordinates at the start of the interception, i.e., $\boldsymbol{e}_r = \boldsymbol{i}, \boldsymbol{e}_\theta = \boldsymbol{j}$, and $\boldsymbol{e}_\phi = \boldsymbol{k}$ (see Fig. 2). Hence, at the beginning of interception Eq. (47) is reduced to Eq. (51). As the interception proceeds, η is changing from η_0 and the spherical coordinates $(\boldsymbol{e}_r, \boldsymbol{e}_\theta, \boldsymbol{e}_\phi)$ rotate continuously in such a way that the orientation of $\boldsymbol{e}_h = -\sin\eta\boldsymbol{e}_\theta + \cos\eta\boldsymbol{e}_\phi$ keeps fixed in the space, as depicted in Fig. 2.

IV. Two-Player Game: Three-Dimensional RTPN vs Three-Dimensional IPN

It is not surprising that the results of Eqs. (17–19) are identical to those in Ref. 14 because PN always can be described as a two-dimensional solution for nonmaneuvering targets. For maneuvering targets with general three-dimensional trajectories, however, the relative motion resulted from PN cannot be described by a two-dimensional plane, and in these cases the study of three-dimensional relative motion has its merits. In this section, we consider a three-dimensional RTPN guidance law with a maneuvering target. Instead of assuming an artificial target motion, we examine the air combat game where a missile guided by three-dimensional RTPN is designed to pursue a target guided by three-dimensional IPN. The general analysis framework introduced in Sec. II allows the analysis of these two guidance laws under a unified approach.

IPN is a new guidance scheme with commanded acceleration applied in the direction normal to the relative velocity between missile and target. It is reported[15] in the two-dimensional case that with some more energy consumption, this new guidance scheme has a larger capture region and is much more effective than the other schemes. The commanded acceleration of target according to three-dimensional IPN guidance law has the vector form

$$\begin{aligned}\boldsymbol{a}_T &= -\lambda_T\dot{\boldsymbol{r}} \times \boldsymbol{\Omega}_{M/T} \\ &= \lambda_T\dot{\boldsymbol{r}}(\boldsymbol{h}/r^2) \\ &= \lambda_T(h^2/r^3)\boldsymbol{e}_r - \lambda_T(h\dot r/r^2)\boldsymbol{e}_h^\perp\end{aligned} \quad (52a)$$

where λ_T is the navigation constant of target and $\boldsymbol{\Omega}_{M/T}$ is the angular rate of LOS as observed from target. The minus sign in Eq. (52a) means that the effort of the target is to increase the LOS rate.

According to the definition of three-dimensional RTPN, the commanded missile acceleration $\boldsymbol{a}_M$ is given by Eq. (15):

$$\begin{aligned}\boldsymbol{a}_M &= \lambda_M\dot r\boldsymbol{e}_r \times \boldsymbol{\Omega}_{T/M} \\ &= \lambda_M\dot r\boldsymbol{e}_r(\boldsymbol{h}/r^2) \\ &= -\lambda_M(h\dot r/r^2)\boldsymbol{e}_h^\perp\end{aligned} \quad (52b)$$

where λ_M is the navigation constant of the missile and $\boldsymbol{\Omega}_{T/M}$ is the angular rate of LOS between the target and missile as observed by the missile. The effort of the missile is to decrease the LOS rate. Comparing Eq. (52b) with Eq. (52a), we can see that IPN has an additional acceleration component that provides IPN with additional freedom of motion. This explains why IPN is much more effective.

The relative acceleration becomes

$$\begin{aligned}\boldsymbol{a} &= \boldsymbol{a}_T - \boldsymbol{a}_M \\ &= \lambda_T(h^2/r^3)\boldsymbol{e}_r + (\lambda_M - \lambda_T)(h\dot r/r^2)\boldsymbol{e}_h^\perp\end{aligned} \quad (53)$$

After substituting Eq. (53) into Eqs. (13), we obtain the set of nonlinear equations describing the two-player game,

$$\ddot r - (h^2/r^3) = \lambda_T(h^2/r^3) \quad (54a)$$

$$\dot h = (\lambda_M - \lambda_T)h(\dot r/r) \quad (54b)$$

$$\dot{\boldsymbol{e}}_h = 0 \quad (54c)$$

Equations (54) can be solved by the same procedure as given in the preceding section. First, Eqs. (54a) and (54b) are solved together, leading to the following dimensionless forms:

$$\bar h = \bar h_0\rho^{\lambda_M - \lambda_T} \quad (55a)$$

$$\Omega = h/r^2 = \Omega_0\rho^{\lambda_M - \lambda_T - 2} \quad (55b)$$

$$\frac{\mathrm{d}\rho}{\mathrm{d}\tau} = -\sqrt{\frac{\dot r_0^2}{V_0^2} - \frac{(\lambda_T+1)\bar h_0^2}{\lambda_M - \lambda_T - 1} + \frac{(\lambda_T+1)\bar h_0^2\rho^{2(\lambda_M-\lambda_T-1)}}{\lambda_M - \lambda_T - 1}} \quad (55c)$$

To maintain the finite acceleration requirement, the navigation constant of missile λ_M has to satisfy

$$\lambda_M > \lambda_T + 2 \quad (56)$$

Initial conditions that guarantee successful interception can be derived from Eq. (55c):

$$\frac{|\dot r_0|/V_0}{\bar h_0} > \sqrt{\frac{\lambda_T + 1}{\lambda_M - \lambda_T - 1}} \quad (57a)$$

or, equivalently,

$$\bar h_0 < \sqrt{1 - [(\lambda_T + 1)/\lambda_M]} \quad (57b)$$

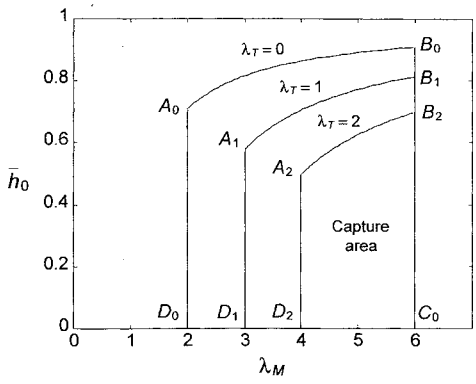

Fig. 3 Capture area for target maneuvering by three-dimensional IPN.

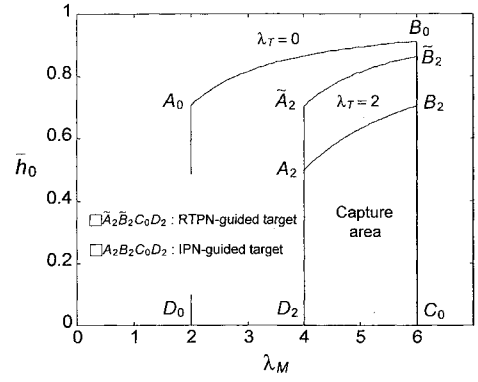

Fig. 4 Capture area for target maneuvering by three-dimensional RTPN and three-dimensional IPN.

by noting that $\sqrt{[\bar{h}_0^2 + (\dot{r}_0/V_0)^2]} = 1$. The capture region defined by Eqs. (56) and (57b) is depicted in Fig. 3, where the upper bound of λ_M is set equal to 6 to avoid instability caused by time lags and noise. As expected, the capture area is narrowed gradually when λ_T increases. If $\lambda_T = 0$, Eq. (57b) reduces automatically to Eq. (22), which is the capture area of three-dimensional RTPN with a nonmaneuvering target. As for the case where a RTPN-guided missile pursues a RTPN-guided target, the corresponding capture region is given by

$$\bar{h}_0 < \sqrt{1 - [1/(\lambda_M - \lambda_T)]} \tag{58}$$

This region is compared with the already given capture region for the IPN-guided missile in Fig. 4. It is observed that the capture region defined by Eq. (58) is larger than the region defined by Eq. (57b) by noting that

$$\sqrt{1 - [1/(\lambda_M - \lambda_T)]} > \sqrt{1 - [(\lambda_T + 1)/\lambda_M]}$$

This observation reveals the fact that the IPN-guided target is harder to intercept than the RTPN-guided target.

Equation (55c) is integrated to get the relation between normalized time τ and range to go ρ,

$$\tau = -\int_1^{\rho} \frac{\mathrm{d}\rho}{\sqrt{\left(\dot{r}_0^2/V_0^2\right) - \left[(\lambda_T + 1)\bar{h}_0^2/(\lambda_M - \lambda_T - 1)\right] + \left[(\lambda_T + 1)\bar{h}_0^2\rho^{2(\lambda_M - \lambda_T - 1)}/(\lambda_M - \lambda_T - 1)\right]}} \tag{59}$$

The duration of interception τ_f can be obtained by setting $\rho = 0$ in the upper limit of the preceding integration. The commanded missile acceleration for a RTPN-guided missile pursuing an IPN-guided target can be evaluated from Eq. (52b):

$$\frac{a_M}{V_0^2/r_0} = \lambda_M \bar{h}\rho^{-2}\left(\frac{\mathrm{d}\rho}{\mathrm{d}\tau}\right) = \lambda_M \bar{h}_0\rho^{\lambda_M - \lambda_T - 2}$$

$$\times\sqrt{\frac{\dot{r}_0^2}{V_0^2} - \frac{(\lambda_T + 1)\bar{h}_0^2}{\lambda_M - \lambda_T - 1} + \frac{(\lambda_T + 1)\bar{h}_0^2\rho^{2(\lambda_M - \lambda_T - 1)}}{\lambda_M - \lambda_T - 1}} \tag{60}$$

The total normalized cumulative velocity increment ΔV required by the RTPN-guided missile pursuing a IPN-guided target is calculated by integrating Eq. (60) with the help of Eq. (55c):

$$\begin{aligned}\Delta V &= \int_0^{\tau_f} \left|\frac{a_M}{V_0^2/r_0}\right| \mathrm{d}\tau \\ &= \int_0^1 \lambda_M \bar{h}_0\rho^{\lambda_M - \lambda_T - 2}\,\mathrm{d}\rho \\ &= \frac{\lambda_M}{\lambda_M - \lambda_T - 1}\bar{h}_0\end{aligned} \tag{61}$$

On the other hand, the total normalized cumulative velocity increment ΔV required by the RTPN-guided missile pursuing an RTPN-guided target is found as

$$\Delta V = \frac{\lambda_M - \lambda_T}{\lambda_M - \lambda_T - 1}\bar{h}_0 \tag{62}$$

Comparing Eq. (61) with Eq. (62), we can see that much more energy consumption is required to intercept an IPN-guided target.

The preceding discussions all result from the solution of Eqs. (54a) and (54b). The remaining problem is to solve Eq. (54c). Since Eq. (54c) is identical to Eq. (16c), the solutions obtained from Eqs. (30–33) are still valid for the case of maneuvering targets. Solving $\mathrm{d}\theta/\mathrm{d}\tau$ and $\mathrm{d}\phi/\mathrm{d}\tau$ from Eqs. (32), (33), and (55a), we obtain

$$\frac{\mathrm{d}\theta}{\mathrm{d}\tau} = \frac{\bar{h}_0\rho^{\lambda_M - \lambda_T - 2}}{l\cos^2\phi} \tag{63a}$$

$$\frac{\mathrm{d}\phi}{\mathrm{d}\tau} = \bar{h}_0\rho^{\lambda_M - \lambda_T - 2}\sqrt{1 - l^{-2}\cos^{-2}\phi} \tag{63b}$$

Combining Eqs. (55c) and (63b) yields

$$\int_0^{\phi} \frac{\mathrm{d}\phi}{\sqrt{1 - l^{-2}\cos^{-2}\phi}} = \int_{\rho}^1 \frac{\bar{h}_0\rho^{\lambda_M - \lambda_T - 2}\mathrm{d}\rho}{\sqrt{\left(\dot{r}_0^2/V_0^2\right) - \left[(\lambda_T + 1)\bar{h}_0^2/(\lambda_M - \lambda_T - 1)\right] + \left[(\lambda_T + 1)\bar{h}_0^2\rho^{2(\lambda_M - \lambda_T - 1)}/(\lambda_M - \lambda_T - 1)\right]}} \tag{64}$$

As in the case of nonmaneuvering targets, here we introduce two auxiliary azimuths η and ψ to simplify the derivation. The auxiliary azimuth η is defined in the same way as Eq. (40) and the relation between θ and η is also given by Eq. (45). The other auxiliary azimuth ψ is defined as

$$\frac{\cos\psi}{\cos\psi_0} = \rho^{\lambda_M - \lambda_T - 1} \tag{65}$$

where $\psi_0 = \cos^{-1} B$, with B defined by

$$B = \frac{\bar{h}_0}{|\dot{r}_0|/V_0}\sqrt{\frac{\lambda_T + 1}{\lambda_M - \lambda_T - 1}} \tag{66}$$

It is easy to verify that the capture region defined in Eq. (57b) is equivalent to the condition $B < 1$. We can use ψ and η to express $\bar{h}, \phi, \theta, \ldots$, and so on. For example, from Eqs. (55a) and (65), we have

$$\frac{\bar{h}}{\bar{h}_0} = \left(\frac{\cos\psi}{\cos\psi_0}\right)^{[(\lambda_M-\lambda_T)/(\lambda_M-\lambda_T-1)]} \tag{67}$$

Using Eq. (65) in Eq. (64), we obtain the expression for ϕ,

$$\phi = \sin^{-1}\left\{\sin\eta_0 \sin\left[\frac{\sinh^{-1}\cot\psi_0 - \sinh^{-1}(\cos\psi/\sin\psi_0)}{\sqrt{(\lambda_M-\lambda_T-1)(\lambda_T+1)}}\right]\right\} \tag{68}$$

Finally, the required time of interception is evaluated by substituting Eq. (65) into Eq. (59):

$$\tau_f = \frac{1}{|\dot{r}_0|/V_0}\int_0^1 \frac{\mathrm{d}\rho}{\sqrt{\sin^2\psi_0 + \cos^2\psi_0\rho^{2(\lambda_M-\lambda_T-1)}}} \tag{69}$$

V. Analytical and Numerical Results

The analytical solution of the nonlinear differential equations describing the motion of a three-dimensional RTPN-guided missile pursuing a three-dimensional IPN-guided target is summarized as follows.

1) The three second-order nonlinear differential equations to be solved are Eqs. (1) with the missile acceleration and target acceleration given by Eqs. (52b) and (52a), respectively,

$$\ddot{r} - (\lambda_T+1)r\dot{\phi}^2 - (\lambda_T+1)r\dot{\theta}^2\cos^2\phi = 0 \tag{70a}$$

$$r\ddot{\theta}\cos\phi - (\lambda_M-\lambda_T-2)\dot{r}\dot{\theta}\cos\phi - 2r\dot{\theta}\dot{\phi}\sin\phi = 0 \tag{70b}$$

$$r\ddot{\phi} - (\lambda_M-\lambda_T-2)\dot{r}\dot{\phi} + r\dot{\theta}^2\cos\phi\sin\phi = 0 \tag{70c}$$

where $\lambda_T = 0$ corresponds to a nonmaneuvering target.

2) The six initial conditions are given by $r_0, \dot{r}_0, \theta_0, \dot{\theta}_0, \phi_0$, and $\dot{\phi}_0$. Without loss of generality, we choose the inertial reference line as the initial LOS and choose the directions of the spherical coordinates such that $\theta_0 = \phi_0 = 0$, $\dot{\theta}_0 > 0$, and $\dot{\phi}_0 > 0$.

3) The various integration constants are determined from the following relations:

$$h_0 = r_0\sqrt{\dot{\phi}_0^2+\dot{\theta}_0^2} \qquad V_0 = \sqrt{\dot{r}_0^2 + r_0^2(\dot{\phi}_0^2+\dot{\theta}_0^2)} \tag{71a}$$

$$\bar{h}_0 = \frac{r_0\sqrt{\dot{\phi}_0^2+\dot{\theta}_0^2}}{\sqrt{\dot{r}_0^2 + r_0^2(\dot{\phi}_0^2+\dot{\theta}_0^2)}} \qquad l = \sqrt{\frac{\dot{\phi}_0^2+\dot{\theta}_0^2}{\dot{\theta}_0^2}} \tag{71b}$$

$$\psi_0 = \cos^{-1}\sqrt{\frac{\bar{h}_0^2(\lambda_T+1)}{(1-\bar{h}_0^2)(\lambda_M-\lambda_T-1)}} \qquad \eta_0 = \cos^{-1}\left(\frac{1}{l}\right) \tag{71c}$$

4) At any instantaneous normalized range to go $\rho = r/r_0$, determine the auxiliary azimuth ψ from Eq. (65).

5) Determine the azimuth ϕ from the auxiliary azimuth ψ via Eq. (68).

6) Determine the auxiliary azimuth η from the azimuth ϕ via Eq. (40).

7) Determine the azimuth θ from the auxiliary azimuth η via Eq. (45).

8) Determine the normalized forward time τ from the normalized range ρ via Eq. (69).

The analysis of the three-dimensional RTPN guidance law can be greatly simplified by using the explicit formulas. Some inherent properties of the three-dimensional RTPN, gained from numerical results, are discussed in the following.

A. Influence of Navigation Constant

Figures 5–8 show the variations of Ω, $\mathrm{d}\rho/\mathrm{d}\tau$, ϕ, and θ with respect to the dimensionless relative distance ρ for various values of navigation constant λ and for various initial conditions. The relative motions can be divided into three categories according to the value of λ.

1) Divergent relative motion is when $\lambda < 2$; the angular rate of LOS, the azimuths θ and ϕ, and the maximum required missile acceleration all grow without bound, indicating a failure of interception.

2) Steady-state relative motion is when $\lambda = 2$; from Eq. (19), we have $\Omega = \Omega_0 = \text{const}$. In this case, the missile approaches the target steadily, and the required interception time is evaluated from Eq. (26) as

$$\tau_f = \frac{\ell_n\cot(\psi_0/2)}{\bar{h}_0}$$

3) Convergent relative motion is when $\lambda > 2$; all of the physical variables converge as the collision point is approaching, and the converging speed of the relative motion increases as λ is increased.

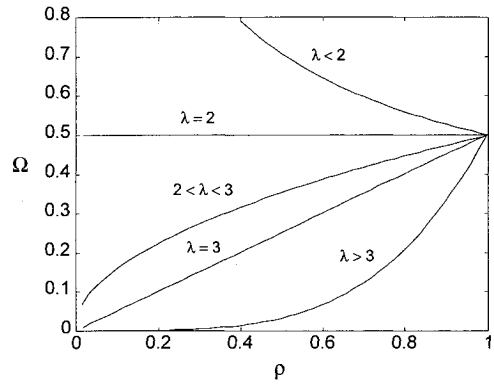

Fig. 5 Angular rate for LOS: $\bar{h}_0 = 0.5$.

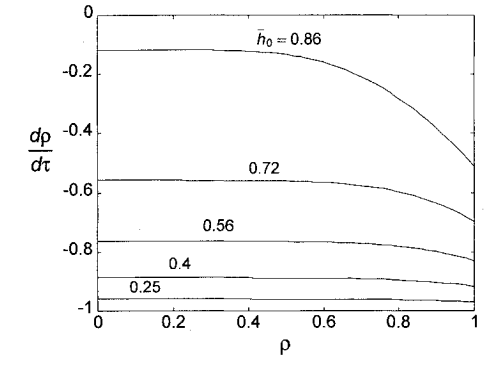

Fig. 6 Closing speed for three-dimensional RTPN: $\lambda = 4$.

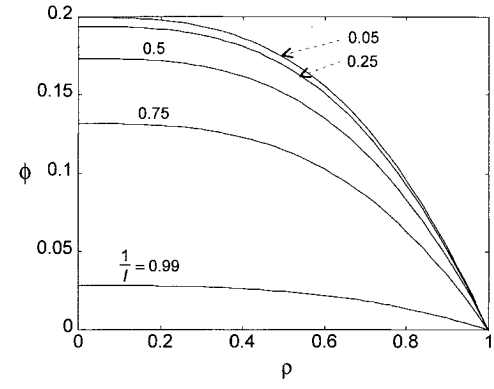

Fig. 7 Azimuth angle ϕ for three-dimensional RTPN with varying l: $\lambda = 4$ and $\bar{h}_0 = 0.5$.

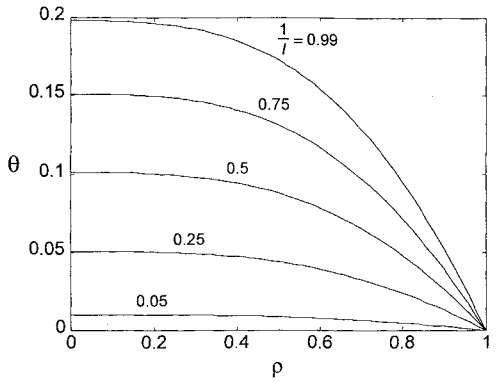

Fig. 8 Azimuth angle θ for three-dimensional RTPN with varying l: $\lambda = 4$ and $\bar{h}_0 = 0.5$.

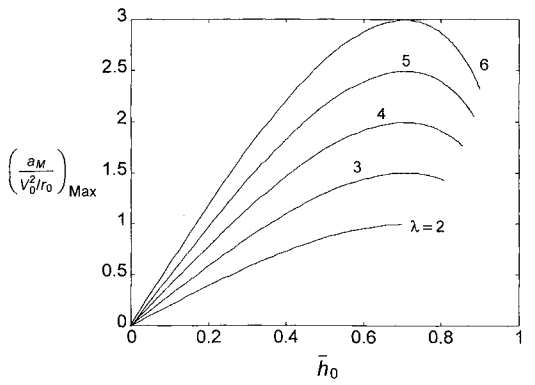

Fig. 9 Maximum acceleration vs initial angular momentum.

B. Influence of Initial Conditions

The analytical solutions in dimensionless form are determined uniquely by two parameters $\bar{h}_0$ and l (ψ_0 and η_0, equivalently) that have the following physical interpretation as can be seen from Eqs. (71b):

$$\bar{h}_0 = \frac{r_0\sqrt{\dot{\phi}_0^2 + \dot{\theta}_0^2}}{\sqrt{\dot{r}_0^2 + r_0^2\left(\dot{\phi}_0^2 + \dot{\theta}_0^2\right)}} = \frac{\text{tangential relative velocity}}{\text{total relative velocity}}$$

$$l^{-1} = \sqrt{\frac{\dot{\theta}_0^2}{\dot{\phi}_0^2 + \dot{\theta}_0^2}} = \frac{\text{tangential velocity in the } \theta \text{ direction}}{\text{total tangential velocity}}$$

Hence, as $l^{-1} \to 1$, the target is escaping in the θ direction initially. In this case, the azimuth θ undergoes large variation (see Fig. 8), while the azimuth ϕ is nearly constant (see Fig. 7). On the other hand, as $l^{-1} \to 0$, the target's initial evasion is along the ϕ direction. In this case, the azimuth ϕ undergoes large variation (see Fig. 7), while the azimuth θ is nearly constant (see Fig. 8).

Next, we consider the effect of $\bar{h}_0$. As $\bar{h}_0 \to 1$, the target is escaping initially almost along the tangential direction, resulting in a large maneuver in the ϕ and θ directions and necessitating large commanded missile acceleration and large energy consumption (see Figs. 9 and 11, respectively), and requiring longer time to pursue (see Fig. 10); while $\bar{h}_0 \to 0$, the target is escaping initially almost along the radial (LOS) direction, and very small missile acceleration is required (see Fig. 9). In the case of $\bar{h}_0$ near 0, the influence of navigation constant is quite insignificant. But when $\bar{h}_0$ approaches the boundary of the capture area, as shown in Fig. 3, a large navigation constant can remarkably improve the efficiency of interception. In the preceding numerical simulations, the value of $\bar{h}_0$ may not cover the full range between 0 and 1, since $\bar{h}_0$ must be restricted to the capture area depicted in Fig. 3 for a successful interception.

There is a simple expression for the largest commanded acceleration of a RTPN-guided missile. From Eq. (60), we see that the largest commanded missile acceleration occurs at $\rho = 1$, i.e., at the beginning of the interception. Hence,

$$\left(\frac{a_M}{V_0^2/r_0}\right)_{\max} = \lambda_M \bar{h}_0\sqrt{1 - \bar{h}_0^2}$$

This expression is valid for both nonmaneuvering and maneuvering targets guided by three-dimensional IPN. Among all possible values of $\bar{h}_0$, we have

$$\max_{0 \le \bar{h}_0 \le 1}\left(\frac{a_M}{V_0^2/r_0}\right)_{\max} = \frac{\lambda_M}{2}$$

and the maximum is achieved at $\bar{h}_0 = 1/\sqrt{2}$ (see Fig. 9).

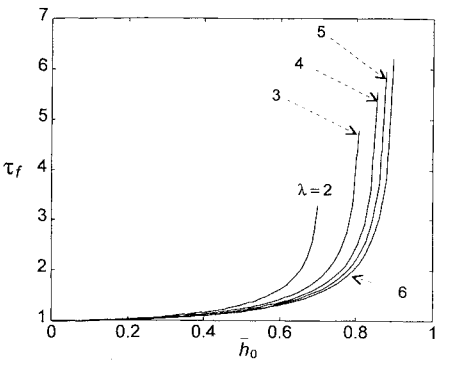

Fig. 10 Time of interception vs initial angular momentum.

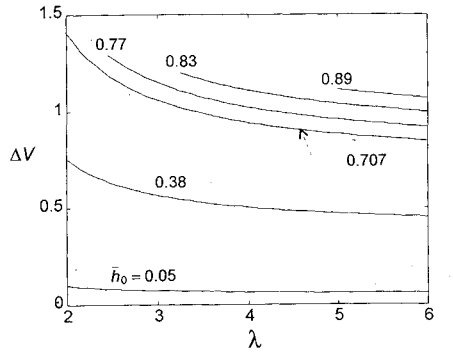

Fig. 11 Energy cost for nonmaneuvering target.

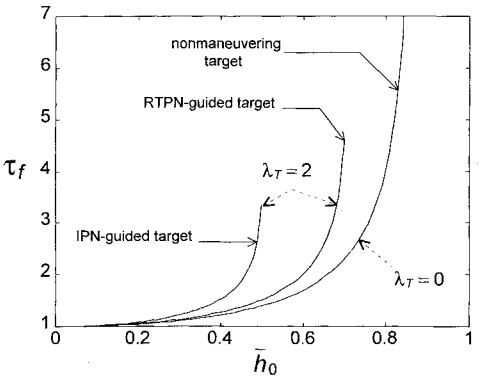

Fig. 12 Time of interception for maneuvering target.

C. Maneuvering Target

In this section, we consider the motion of a three-dimensional RTPN-guided missile pursuing two kinds of maneuvering targets. One is an IPN-guided target and the other is a RTPN-guided target. The capture areas of these two targets have been compared in Fig. 4. The required time of interception τ_f and the required energy consumption for both targets are shown in Figs. 12 and 13, respectively. From these figures, we can see that for IPN-guided targets 1) the

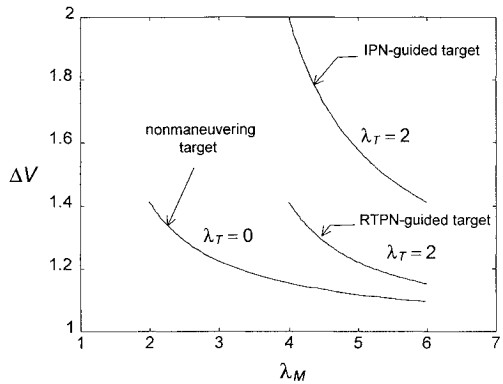

Fig. 13 Energy cost for maneuvering target.

capture area is smaller, 2) the required time of interception is longer, and 3) the required energy consumption of missile is larger.

VI. Conclusions

This paper is devoted to the study of three-dimensional pursuit–evasion motion. Three second-order nonlinear differential equations that describe the motion of missiles guided by three-dimensional realistic true proportional navigation are solved analytically without any linearization. Trajectory and performance analysis are described in terms of the unit angular momentum defined for the relative motion and the success of the RTPN guidance law strongly depends on the initial value of this unit angular momentum. In the two-player game analysis, the IPN-guided targets, as compared with the RTPN-guided targets, are much harder to intercept, with larger required energy consumption of the missile and longer time of interception, as well as with smaller capture area.

Acknowledgment

This research was supported by the National Science Council under Grant NSC84-2212-E-006-107.

References

[1]Murtaugh, S. A., and Criel, H. E., "Fundamental of Proportional Navigation," *IEEE Spectrum*, Vol. 3, Dec. 1966, pp. 75–85.

[2]Guelman, M., "A Qualitative Study of Proportional Navigation," *IEEE Transactions on Aerospace and Electronic Systems*, Vol. AES-7, July 1971, pp. 638–643.

[3]Guelman, M., "Proportional Navigation with a Maneuvering Target," *IEEE Transactions on Aerospace and Electronic Systems*, Vol. AES-8, May 1972, pp. 364–371.

[4]Guelman, M., "Missile Acceleration in Proportional Navigation," *IEEE Transactions on Aerospace and Electronic Systems*, Vol. AES-9, May 1973, pp. 462, 463.

[5]Guelman, M., "The Closed Form Solution of True Proportional Navigation," *IEEE Transactions on Aerospace and Electronic Systems*, Vol. AES-12, July 1976, pp. 472–482.

[6]Yang, C. D., Yeh, F. B., and Chen, C. H., "The Closed-Form Solution of Generalized Proportional Navigation," *Journal of Guidance, Control, and Dynamics*, Vol. 10, No. 2, 1987, pp. 216–218.

[7]Yang, C. D., and Yeh, F. B., "Closed-Form Solution of a Class of Guidance Laws," *Journal of Guidance, Control, and Dynamics*, Vol. 10, No. 4, 1987, pp. 412–415.

[8]Yang, C. D., Hsiao, F. B., and Yeh, F. B., "Generalized Guidance Law for Homing Missiles," *IEEE Transactions on Aerospace and Electronic Systems*, Vol. AES-25, March 1989, pp. 197–212.

[9]Shukla, U. S., and Mahapatra, P. R., "Optimalization of Biased Proportional Navigation," *IEEE Transactions on Aerospace and Electronic Systems*, Vol. AES-25, Jan. 1989, pp. 73–80.

[10]Shukla, U. S., and Mahapatra, P. R., "The Proportional Navigation Dilemma—Pure or True," *IEEE Transactions on Aerospace and Electronic Systems*, Vol. AES-26, March 1990, pp. 382–392.

[11]Mahapatra, P. R., and Shukla, U. S., "Accurate Solution of Proportional Navigation for Maneuvering Targets," *IEEE Transactions on Aerospace and Electronic Systems*, Vol. AES-25, Jan. 1989, pp. 81–89.

[12]Becker, K., "Closed-Form Solution of Pure Proportional Navigation," *IEEE Transactions on Aerospace and Electronic Systems*, Vol. AES-26, April 1990, pp. 526–533.

[13]Yuan, P. J., and Chern, J. S., "Analytic Study of Biased Proportional Navigation," *Journal of Guidance, Control, and Dynamics*, Vol. 15, No. 1, 1992, pp. 185–190.

[14]Yuan, P. J., and Chern, J. S., "Solutions of True Proportional Navigation for Maneuvering and Nonmaneuvering Targets," *Journal of Guidance, Control, and Dynamics*, Vol. 15, No. 1, 1992, pp. 268–271.

[15]Yuan, P. J., and Chern, J. S., "Ideal Proportional Navigation," *Journal of Guidance, Control, and Dynamics*, Vol. 15, No. 5, 1992, pp. 1161–1165.

[16]Yuan, P. J., and Chern, J. S., "Exact Closed-Form Solution of Generalized Proportional Navigation," *Journal of Guidance, Control, and Dynamics*, Vol. 16, No. 5, 1993, pp. 963–966.

[17]Dhar, A., and Ghose, D., "Capture Region for a Realistic TPN Guidance Law," *IEEE Transactions on Aerospace and Electronic Systems*, Vol. AES-29, July 1993, pp. 995–1003.

[18]Ghose, D., "True Proportional Navigation with Maneuvering Target," *IEEE Transactions on Aerospace and Electronic Systems*, Vol. AES-30, Jan. 1994, pp. 229–237.

[19]Ghose, D., "Capture Region for True Proportional Navigation Guidance with Nonzero Miss-Distance," *Journal of Guidance, Control, and Dynamics*, Vol. 17, No. 3, 1994, pp. 627, 628.

[20]Ghose, D., "On the Generalization of True Proportional Navigation," *IEEE Transactions on Aerospace and Electronic Systems*, Vol. AES-30, April 1994, pp. 545–555.

[21]Adler, F. P., "Missile Guidance by Three-Dimensional Proportional Navigation," *Journal of Applied Physics*, Vol. 27, May 1956, pp. 500–507.

[22]Shinar, J., Rotsztein, Y., and Bezner, E., "Analysis of Three-Dimensional Optimal Evasion with Linearized Kinematics," *Journal of Guidance and Control*, Vol. 2, No. 5, 1979, pp. 353–360.

[23]Guelman, M., and Shinar, J., "Optimal Guidance Law in the Plane," *Journal of Guidance, Control, and Dynamics*, Vol. 7, No. 4, 1984, pp. 471–476.

[24]Cochran, J. E., No, T. S., and Thaxton, D. G., "Analytical Solutions to a Guidance Problem," *Journal of Guidance, Control, and Dynamics*, Vol. 14, No. 1, 1991, pp. 117–122.

[25]Yang, C. D., and Yang, C. C., "Analytical Solution of Generalized 3D Proportional Navigation," *Proceedings of the 34th Conference on Decision and Control* (New Orleans, LA), 1995, pp. 3974–3979.

[26]Cloutier, J. R., Evers, J. H., and Feeley, J. J., "Assessment of Air-to-Air Missile Guidance and Control Technology," *IEEE Control Systems Magazine*, Oct. 1989, pp. 27–34.